DEMYSTIFYING ACCRETIONARY PRISM IN THE ANDAMAN BASIN WITH MODERN SEISMIC DATA

Dr. Ritesh Mohan Joshi, Dilip Kumar Mahata &, Mukiri Bhagyakishore*
*Oil India Limited, Kakinada, (AP); *Email: RITESH.JOSHI@OILINDIA.IN*

Keywords: Andaman, seismic, accretionary prism.

Summary

In an unwavering pursuit of discovering new hydrocarbon reserves, Oil India Ltd (OIL), a Navratana category Government of India Enterprise, acquired, processed, and interpreted two-dimensional (2D) seismic data in OALP shallow offshore block situated along the Western coast of the Andaman Main Islands. OIL's return to offshore exploration in the Andaman-Nicobar Basin marks a significant milestone after a hiatus spanning several decades. Accompanied by Shearwater's cutting-edge research vessel, SW Vespucci, extensive and exceptionally rich and high-quality 2D seismic data running in thousands of LKM was meticulously acquired, covering water depths ranging from 0 meters to an impressive 500 meters.

This block area is in the shallow water part of the Andaman-Nicobar basin and is mostly unexplored, with very scanty or no seismic data and a solitary well. In this campaign, the Operator (OIL) acquired, processed and interpreted rich and high-quality data and revealed the best possible subsurface images of target plays of Paleogene and possible Cretaceous sediments. OIL's endeavour is to drill and establish the hydrocarbon potential of this exciting frontier area.

The primary objective of this campaign is to delineate the subsurface structure correctly and to use the improved structural information to explore the processes of accretion. The survey reveals small as well as larger features which were never appreciated before. The acquired 2D seismic data have imaged totally overlapping thrust horses that are characterized by a coincident trailing branch line, off-scraped sediment patterns, and both duplexing and out-of-sequence faulting. The frequent dramatic variation of fault spacing and reflector geometry over a space of several hundred meters is prevalent throughout the area. This is the Andaman accretionary prism which exhibits the geometries of an antiformal stack that contains inclined and stacked thrust horses that are bounded by the main fault traces. Interestingly, none of these variations are associated with detectable changes in the morphology of the underlying envisaged basement. The architecture defined by fault surface reflections is probably controlling gross fluid motion through the prism. The slope sediments account for numerous stages of deformation. Plentiful small offset reverse faults also indicate possible recent shortening of the underlying prism. The key results of this survey improved understanding of the structural assortment throughout the Andaman accretionary prism.

1.0 Introduction

The Andaman-Nicobar Basin is part of a large geotectonic unit that extends from the Indonesian Islands in the south to Myanmar in the north. The basin extends ~1,200 km from Myanmar to Sumatra and ~650 km from the Malay Peninsula to the Andaman and Nicobar Islands (Mohan et. al., 2006). In addition to Andaman and Nicobar Islands, the basin is marked by several prominent geomorphological features, such as Ritchie's Archipelago, Barren and Narcondam volcanic islands, Invisible bank, and Alcock and Sewell seamount complexes (Sewell, 1925a) (Figure 1).

Imaging the subsurface for an accretionary prism is always challenging using 2D seismic data. Because the accretion process involves the off-scraping of rocks and sediments at the front of the prism, stacking of deformed sediments into thick vertical piles, horizontal shortening, fluids expulsion, and the sediment's transformation to rocks (Figure 2). Severely deformed, disrupted, and mixed rocks form melanges. The bulldozer-fashioned, skimmed-off sediments lack internal coherency and make the area difficult for imaging. The high-relief sediments, whether controlled by submarine landslides, debris flows, turbidity currents, or contourites, also lose structural definition with depth because of continuous tectonic readjustments.

2.0 Geological Settings:

2.1 Geology and Tectonics of Andaman & Nicobar Region (ANR)

The Andaman-Nicobar basin came into existence because of the northward movement and anticlockwise rotation of the Indian Plate and its under-thrusting under the Eurasian plate in the Cretaceous time (Figure 3). As subduction progressed, the Outer High Arc complex started rising steeply, thereby creating a depression or a Fore Arc basin between Volcanic Arc and the Outer High Arc due to peripheral bulging. Continued thrusting caused the uplift and formation of the Andaman Nicobar Ridge as a chain of Islands. The Andaman chain of islands forms a part of the geotectonic regime; "The Great Indonesian Island Arc System" of the East Indies and it extends up to Burmese Arc i.e., the Arakan Yoma fold belt.

It is more than 5,000 km in length as per the DGH report for the years between 2012-14.

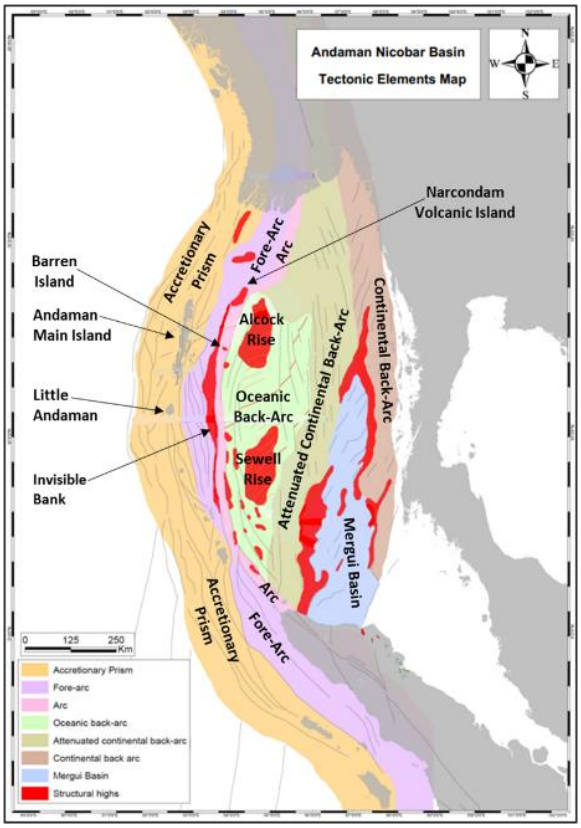

Figure 1: Tectonics of the Andaman Sea region.

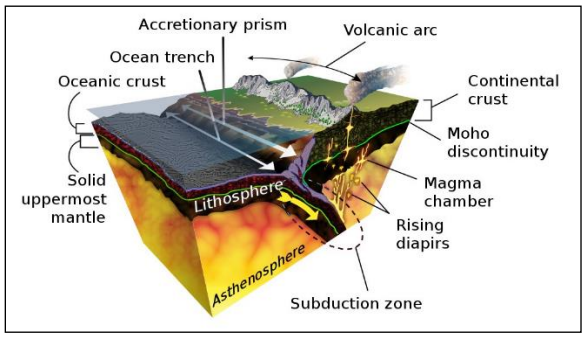

Figure 2: Schematic diagram of various aspects of a subduction zone including accretionary prism (image courtesy: Subduction-en.svg from Wikimedia Commons by K. D. Schroeder, CC-BY-SA 4.0).

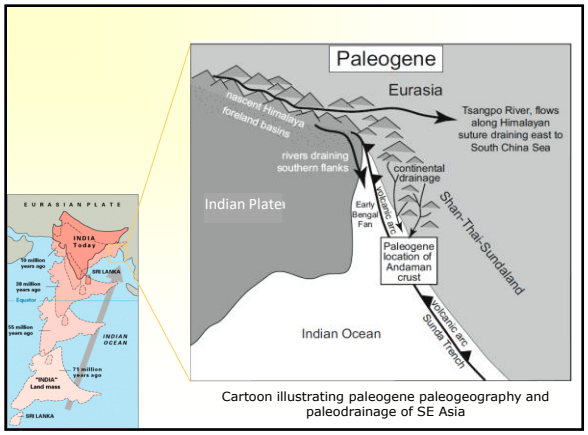

Figure 3: Palaeogene palaeogeography & palaeodrainage of SE Asia

The Andaman-Nicobar basin, a typical island arc system has evolved through a complex history of tectonics associated with the convergent plate boundaries between the Indian plate and west Eurasian plate and northward movement coupled with anticlockwise rotation of the Indian plate. The basin was initiated with the northward drift of the Indian Plate with respect to Asia. The collision of Indian/Eurasian plates initiated along the irregular boundary and occurred at the same time as the oceanic subduction beneath southern Eurasia. The continental collision slowed down the oceanic spreading rates in the Indian Ocean and slowed down the subduction velocity along the Sunda Arc system. Collision processes and subduction of the Indian plate along the Sunda subduction zone resulted in the formation of various tectonic blocks. A spreading centre was also developed in the Back arc basin. The major tectonic elements longitudinally extend from the Java-Sumatra region in the south to the Andaman-Nicobar basin and continue further to the Indo-Myanmar range and central Myanmar basin to the north.

Major Tectonic elements of the Andaman-Nicobar region (Figure 4) are Andaman Trench/Inner slope, Outer High/Trench slope break / Accretionary Wedge, Fore Arc sub-basin, Volcanic Arc, Back Arc Basin, and Mergui Terrace

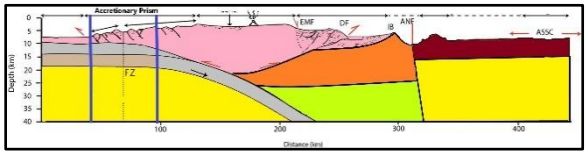

Figure 4: A 2D schematic cross-section of the Andaman–Nicobar subduction system from the oceanic plate to the Andaman Sea spreading center. Note the position of the block vis-e-vie accretionary prism/wedge (Modified after Singh & Moeremans, 2017).

A total of 22 numbers of wells have been drilled in the Andaman-Nicobar basin for oil and gas exploration purposes to date. Most of the wells were drilled targeting primarily the Mid-Miocene sequence and only eight (8) wells have been penetrated up to the Paleogene sequence. The biogenic gas discovery in wells AN-1-1 and ANDW-1 has proven the existence of a shallow biogenic gas petroleum system. The thermogenic system is envisaged to be in nearby areas of the thermogenic source mud volcanoes that existed on Andaman Island.

2.2. Accretionary Prism in Andaman Basin

Geologically, the block area is part of an accretionary wedge and is situated in the outer high/trench slope break of the Andaman-Nicobar Basin at the western side of Andaman main island and east of the trench. The Andaman accretionary prism has formed from sediments accreted onto the Eurasian tectonic plate at the convergent plate boundary along where the Indian plate is subducting. Most of the material in this accretionary wedge consists of marine sediments scraped off from the down-going Indian slab of oceanic crust (Figure 4). The wedge also partially includes the erosional products of volcanic island arcs formed on the overriding plate. The sediments are ocean floor basalts, pelagic sediments, and trench sediments. Trench sediments are typically turbidites possibly derived from oceanic /volcanic island arc, cordilleran orogen, adjacent continental masses located along strike, material transported into the trench by gravity sliding and debris flow from the forearc ridge (olistostrome), and piggy-back basins.

The active tectonic environment has resulted in various types of structural traps in the basin – primarily associated with compression in the accretionary prism. Such traps are anticipated to be the principal type of traps for the accumulation of hydrocarbons in the basin. The presence of good reservoirs is common in trench-slope basins. Subduction zone settings generally offer favourable structural trap scenarios, with active faulting and folding related to accretionary prism growth or trench front erosion. There is a list of productive basins (Hessler and Sharman, 2018) related to intra-oceanic accretionary prism zones and continental subduction zones e.g., Tobago trough (Barbados), Seram Island (Indonesia), Joban and Sagara (both in Japan), Cook Inlet, Sacramento, Cascadia, Franciscan (all four in USA), Talara (Peru), Progreso (Peru-Ecuador) and East-Coast basin (New Zealand). Recent exploration success in the Tayrona-Rancheria basin offshore Colombia is an addition to this series.

3.0 Seismic Survey

In this paper, an attempt has been made to determine the structural disposition of the target area and the configuration of the accretionary prism, a tectonic element of the Andaman-Nicobar basin with the help of suitably acquired and processed (onboard and final) 2D seismic. The onboard data quality control (QC) tools employed during the survey conformed to standard QC deliverables

The acquisition program aimed to conduct shallow water exploratory 2D seismic survey to gain more knowledge of geological structures in the area. The challenges of imaging in accretionary prism by 2D seismic data, due to inherent subsurface complexity, deformed fragmented rocks, and lack of internal coherency was duly considered during the design stage of the survey. The seismic lines were recorded in N-S & E-W direction, also to partially complement the dip-line smear due to reflection point dispersal along the dipping reflector, Few NE-SW lines were also acquired.

The block extends from the North end of Andaman Island down to Sentinel Island. The survey area lies in water depths ranging from 0 m to 500 m. The survey area consisted of many shallow areas and exclusion zones to protect Indigenous people. The acquisition plan included the avoidance of these shallows and restricted areas and was split into two distinct parts to lessen the impact on fishing activities and enhance the operational feasibility.

A six (6) km-long cable was towed behind the seismic vessel at an appropriate depth. Accordingly, the source guns were towed at appropriate depths to acquire the best quality data.

4.0 Results and Discussion

Processing

Shearwater's proprietary Software, Reveal 4.1 was utilized for the processing of the acquired seismic data. The data was processed for both time, depth, and post-stack inversion also performed; however, only time processing is discussed in this paper. The processing steps for time is given in the table below. Besides source and receiver de-ghosting, SRME and SWME are some of the main processing steps for shallow water seismic.

Seismic data processing (Time)

- Linear noise attenuation
- Source and receiver de-ghosting
- De-Signature
- 1st Pass demultiple: SWME
- 2nd Pass demultiple: SRME
- Shot/ Channel scalars
- Receiver motion correction
- Tidal statics correction
- Initial velocity analysis – 1km grid
- Radon demultiple
- Inverse Q compensation (phase only)
- Sort to common offset

- Common offset noise attenuation
- Anisotropic migration vel. analysis: (500 m), eta (4 km)
- Anisotropic pre-stack time migration
- Residual moveout – 4th order, 250 m grid
- Radon demultiple
- Spectral balancing/ inverse Q (amp)
- Angle mute/ Stack
- Spectral balancing
- Post-Stack processing: coherency, denoise, filter, gain

Source & Receiver de-ghosting: Ghosts are introduced from reflections of water surface at both source & receiver side during recording. They introduce notches on the frequency spectra at 0 Hz and at water velocity/2x depth which introduce side-lobes onto the zero-phased wavelet, reducing the resolution for fine beds and introducing tuning effects where horizons converge. In this survey, the 5m source depth & 7m receiver depth resulted in source ghost notch at 150 Hz & receiver ghost notch at 107 Hz.

Receiver de-ghosting was performed by using a 2D f-k algorithm, re-datuming the data to account for the measured receiver depth at each channel. L1 optimization for the receiver depth was applied to improve the precision of the de-ghosting. Source de-ghosting was also performed with a 2D f-k algorithm, using an L1 optimization process to select the best source depth, allowing for a maximum change of +/- 1 m from the recorded depth.

Since de-ghosting boosts bubble energy when infilling the ghost notch at 0 Hz, it is desirable to remove the bubble while testing to assess the total effect on amplitude and phase. To facilitate this, a 1D de-signature filter was applied, prior to full testing of the de-signature. Amplitude spectra and autocorrelations indicated that source and receiver de-ghosting was successfully removing side-lobe energy, providing enhanced resolution. Figure 5a, 5b & 5c represents stack before de-ghosting, stack after receiver de-ghosting and stack after receiver de-ghosting, source de-ghosting and de-signature. Figure 5d represents stack amplitude spectra after receiver-source de-ghosting and 1d de-signature.

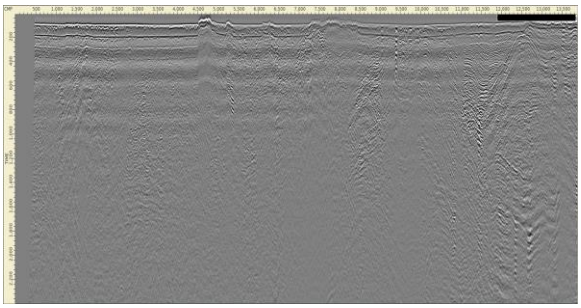

Figure 5 (a): Stack before de-ghosting.

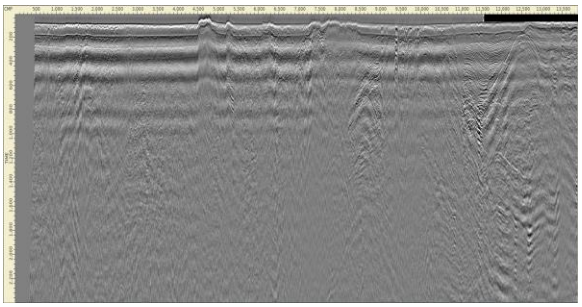

Figure 5 (b) stack after receiver de-ghosting.

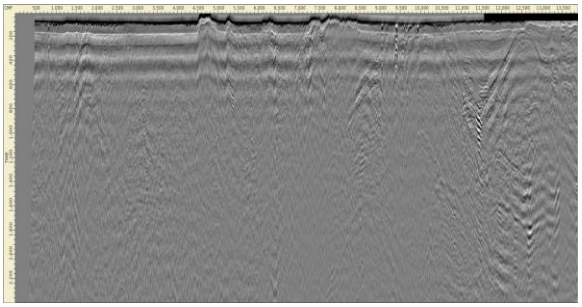

***Figure 5 (c): Stack after receiver de-ghosting, source de-ghosting and* de-signature**

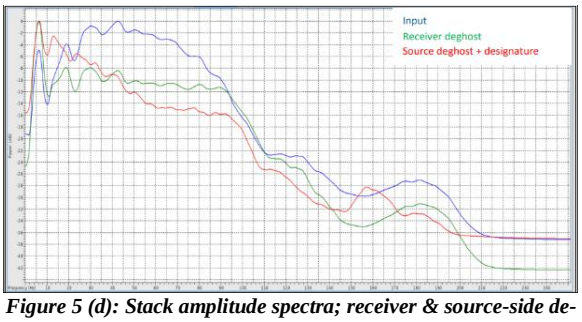

Figure 5 (d): Stack amplitude spectra; receiver & source-side de-ghosting and 1-d de-signature.

Velocity analysis: After line sequence merge and demultiple, initial velocity analysis was performed on every line at one (1) km intervals, the guide function being two (2) km velocities picked on the vessel.

Kirchhoff pre-stack time migration was used to migrate all the lines using the existing 1 km velocity field. The output migrated gathers were used to pick RMS migration velocities at 0.5 km intervals and eta at 4 km intervals. PreSTM requires a laterally smooth velocity field. The picked velocities were smoothed using a 1 km filter in interval slowness and converted back to RMS (Figure 5e & 5f).

2d Anisotropic Kirchhoff Pre-stack time migration: Kirchhoff migration was applied with an operator incorporating anti-alias filters and phase and amplitude correction terms. Migration half-apertures from 3-6 km were tested using a dip limit of 70°. Dip limits from 50°- 70° were tested using a half-aperture of 5 km. Migrating with smaller apertures tends to lead to less residual noise but can degrade steep-dip imaging if too small.

By comparing PreSTM stacks on test lines, it was clear that increasing the aperture to 5 km led to better-resolved events, although more migration noise was apparent using 6 km. Increasing the dip limit to 70° led to clearer fault definition, especially in the shallow areas. Eventually, a five (5) km aperture and 70° dip limit were considered optimum.

It was confirmed by migrating an extracted wavelet and inspecting impulse responses that using phase correction in the PreSTM maintained the zero phase of the data (Figure 5g).

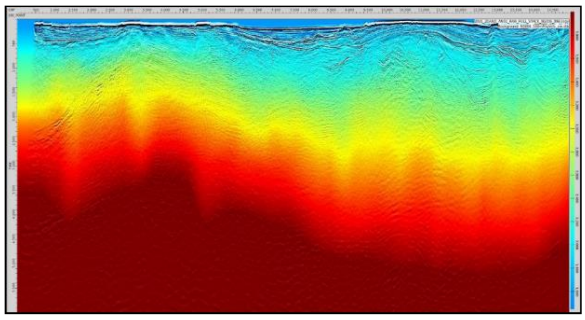

Figure 5 (e): Smoothed PSTM RMS velocities at every 1 Km.

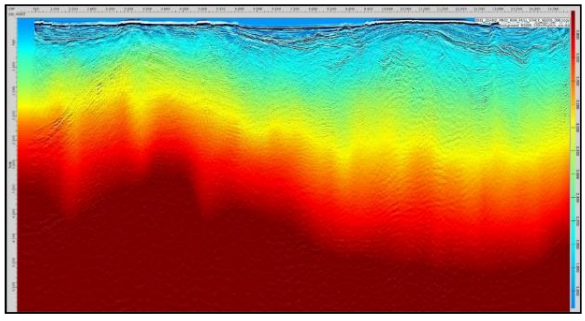

Figure 5 (f) migration velocity analysis at every 500 m.

Full-Fold Stack: Spectral balancing, coherency, denoise, filter & gain was applied as post-processing (Figure 5h).

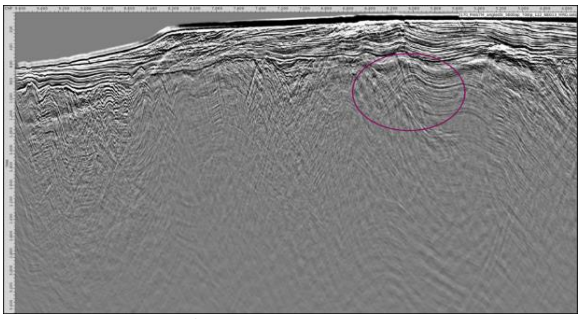

Figure 5 (g): Stack after PreSTM with 5 km aperture and 70° dip limit.

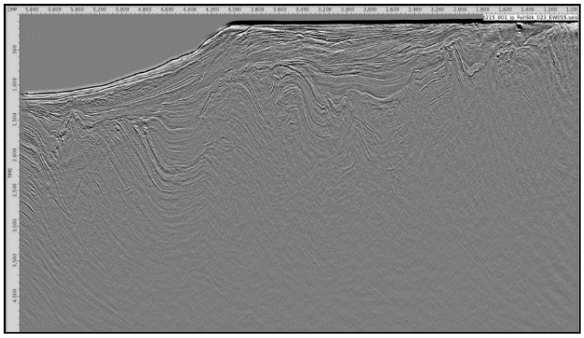

Figure 5 (h): Full-fold stack after migration & post-processing.

The overall data quality for the duration of the survey was extremely high with minimal noise. The only noise of any significance was turn/bend noise as a large percentage of the lines required tight turns onto the line with no run-in resulting in high feather angles. The preliminary noise attenuation run onboard proved that a large amount of the bend noise can be eliminated without signal damage. Shot gathers with the most severe noise and apparent curvature of direct arrivals were rejected during onboard QC. The accepted data posed no issue for further processing.

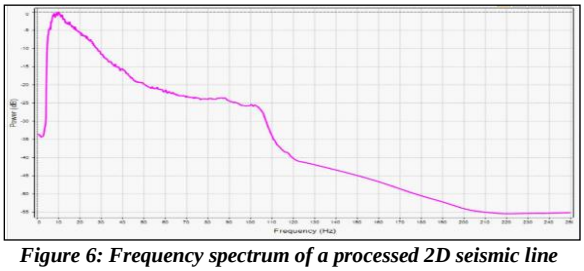

Figure 6: Frequency spectrum of a processed 2D seismic line

Occasional earthquake noise affected a little amount of data. Those shot gathers with high amplitude earthquake noise were flagged as NTBP and were excluded from processing. Water layer back-scattered coherent noise was seen on many lines. This type of noise is normally removed during the normal routine of the linear noise attenuation processing

stage. The ground roll was visible in water depths of less than 20m but generally affected a short range of shot points and its high-angle linear nature made it easy to remove and therefore not a data quality issue. The frequency spectrum of a processed seismic line has been shown in Figure 6.

5.0 Conclusions

From operational and data quality points of view, this survey was a success, although a lot of chaos/uncertainty was there on account of the first wave of Covid. Excellent communication between the navigation department and the bridge crew resulted in safe shooting. Planning was done on a line-by-line basis which maximized coverage. This could not have happened without the effective use of the chase vessels for a plethora of bathymetry verifications. Technical downtime was the lowest possible except for a problematic active section in the streamer and three technical sues. This is probably because of strong reflected energy in extremely shallow waters with areas of very hard water bottom. The acquired seismic turned out to be very good and beautiful accretionary prisms were observed in the seismic sections (Figure 7).

Andaman accretionary prisms are formed by sediments or debris accumulation, and they are easily identified in seismic by fault-bounded wedges of sediment above the descending slab. The variation of seismic reflection suggests that the rheology of Andaman accretionary prisms is possibly varying from a brittle to viscoelastic-plastic nature with increasing depth. Thus, the frontal part of the accretionary prism does not mimic the morphology of the trench ward part of the framework rock. The younger sediments have more influence and increasing thickness trend towards the west of the block. The curvature of the envisaged basement does not correlate with the curvature of the deformation front or toe of the accretionary prism. The age of Individual wedges in the Andaman accretionary prism is expected to be decreasing as the trench is approached. The intensely deformed accretionary prisms produced mélange. The seismic energy has probably dissipated due to a lack of continuous bedding and the inclusion of fragmented rocks. Although Olistostromes mélanges clasts produced by gravitational sliding do not have bedding, the tightly folded mélanges with more than one cleavage or foliation are also mappable in this seismic data acquired over Andaman accretionary prism.

6.0 References

1. Hessler and Sharman, 2018, Subduction zones and their hydrocarbon systems, Geosphere, The Geological Society of America
2. Singh, SC., & Moeremans, R., 2017, Geological Society, London, Memoirs, 47, pp-193-204.
3. Sewell, R.B.S., 1925a. The geography of the Andaman Sea Basin. Mere. Asiatic Soc. Bengal, 9:1-26.
4. DGH Annual report 2013-14.
5. Subduction-en.svg from Wikimedia Commons by K. D. Schroeder, CC-BY-SA 4.0).

7.0 Acknowledgments

The authors are thankful to the management of Oil India Limited for permitting them to present and publish this work. Views expressed in this technical paper are of the authors only.

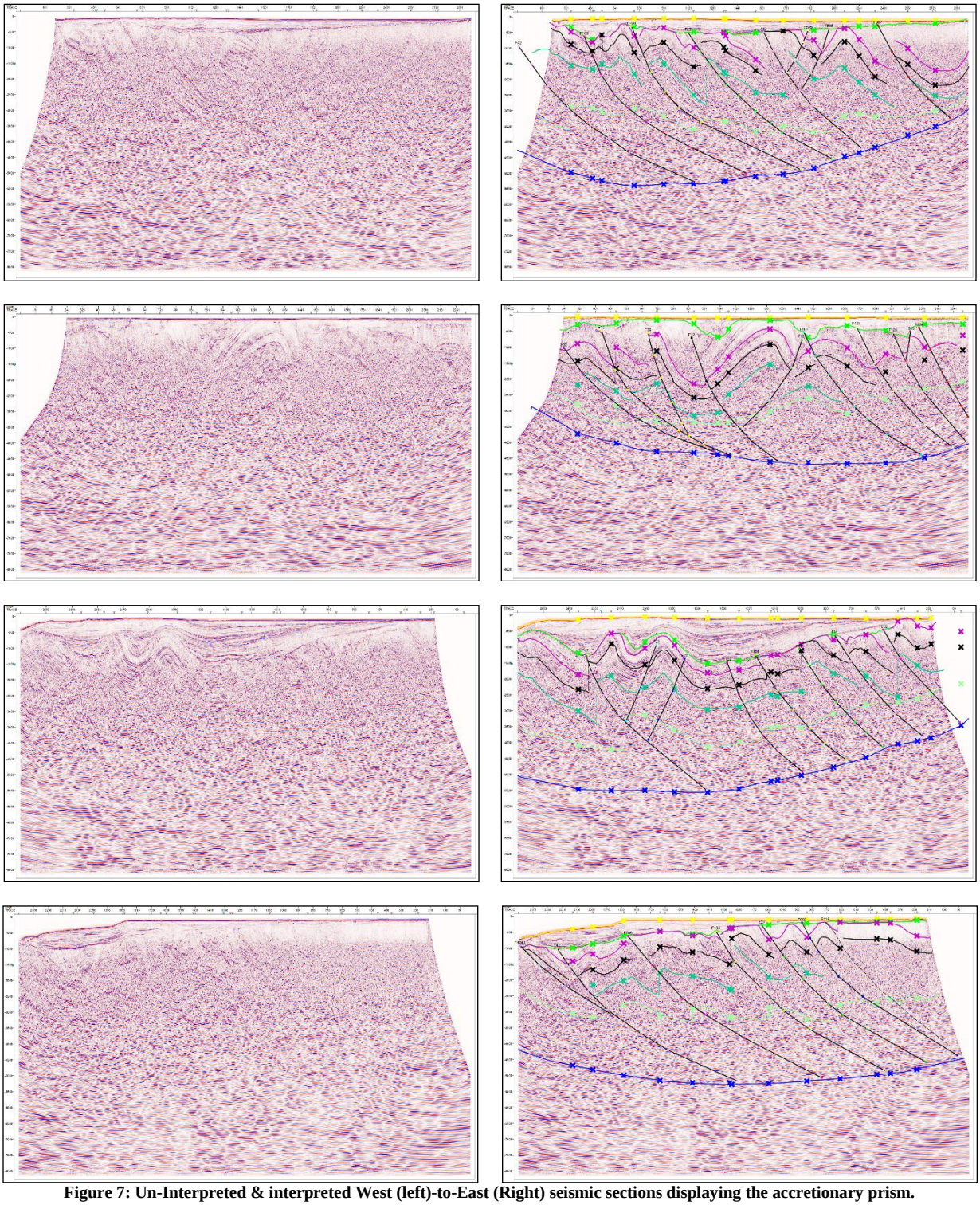

Figure 7: Un-Interpreted & interpreted West (left)-to-East (Right) seismic sections displaying the accretionary prism.